Anal. Bioanal. Electrochem., Vol. 16, No. 7, 2024, 671-682
https://www.doi.org/10.22034/abec.2024.714691

Analytical & Bioanalytical Electrochemistry

Full Paper

Electrocatalytic Oxidation of Ethylene Glycol on Metal-Organic Framework (Ni-BTC)/Multi-Walled Carbon Nanotubes Composite Electrode

Mojtaba Hadi,* Masoumeh Khonjouki, Hossein Mostaanzadeh, and Ali Ehsani

Department of Chemistry, Faculty of Sciences, University of Qom, Qom, Iran

*Corresponding Author, Tel.: +982532103093
E-Mail: m.hadi@qom.ac.ir

Received: 10 May 2024 / Received in revised form: 3 July 2024 /
Accepted: 5 July 2024 / Published online: 31 July 2024

Abstract- In this work, the direct electrochemical oxidation of ethylene glycol (EG) on a nickel-based metal-organic framework (MOF)/multiwall carbon nanotubes (CNTs) hybrid composite electrode was investigated. This investigation is used to verify the possibility of using the Ni-MOF/CNTs electrode in the ethylene glycol fuel cells. The morphology of the composite layer on the surface of the electrode substrate was examined by scanning electron microscopy (SEM). The cyclic voltammetry technique was used to examine the typical electrocatalytic performance of the electrode. In 0.1 M NaOH solution, well-defined oxidation and reduction peaks of Ni^{2+}/Ni^{3+} redox couple were observed. The electrocatalytic current at the Ni-MOF electrode was also studied for comparison with that of the Ni-MOF/CNTs electrode. Owing to the synergetic effect of the MOF and the CNTs, the Ni-MOF/CNTs electrode shows a satisfactory electrocatalytic activity toward the EG electro-oxidation, making it a promising candidate for use as an ideal anode material in direct alkaline alcohol fuel cells.

Keywords- Metal-organic framework; Carbon nanotube; Fuel cell; Ethylene glycol; Electrocatalytic oxidation

1. INTRODUCTION

Fuel cells, as one of the most noteworthy technologies in the future of energy production, have gained the interest of lots of researchers in science and industry. Due to the several advantages of liquid alcohol fuels compared to hydrogen, such as high energy density and easy

handling/storage, alcohol-based fuel cells have continued to attract greater attention over conventional hydrogen-based fuel cells [1]. One of the key influencing factors on the reaction kinetics of alcohols electro-oxidation is the electrode material and during the last decade, several papers dealing with nanostructured electro-catalysts in direct alcohol fuel cells have been published [2]. Compared to acid-direct alcohol fuel cells that usually employ costly platinum-based electro-catalysts, faster kinetics of alcohols electro-oxidation in alkaline electrolytes provides the possibility of developing electro-catalysts based on less-expensive metals in alkaline direct alcohol fuel cells (ADAFCs) [3]. Nickel, as a relatively cheap and earth-abundant transition metal, has recently aroused considerable attention from scientists owing to its high electro-catalytic activity and cost effectiveness. In the past few years, pure nickel [4,5], nickel-based multi-component alloys [6-9], and various nickel-based compounds [10-16] in the form of composite or non-composite materials have been studied as anode electrode materials in ADAFCs. In the present study, a nickel-based metal-organic framework (MOF), Ni-BTC (BTC= *1*, *3*, *5*-benzene tricarboxylate), was synthesized and used in the form of composite with carbon nanotubes (CNTs) (Ni-BTC/CNTs), for the first time, for the anodic oxidation of ethylene glycol.

MOFs have attracted many researchers' attention in recent years due to their high pore volume, controllable structures, and very large surface area. This is because of their exceptional structures, the combination of various metal ions and organic linkers arranged to form highly ordered porous crystalline structures. They show great potential for several applications such as gas adsorption and separation [17], biomedicine delivery [18], and energy storage in batteries and supercapacitors [19]. Owing to their large porosities and redox properties, they can also serve as promising materials to achieve high electrocatalytic performances. It has been shown that they can successfully catalyze many electrochemical reactions such as oxygen reduction, hydrogen evolution, oxygen evolution, CO_2 reduction and etc. [20-23]. More recently, some researches have been focused on their applications as electro-catalyst for alcohol electro-oxidation in ADAFCs. For example, a Cu-based MOF/graphene oxide (GO) has been explained by Noor et al. [24] and a CoCu-MOF/carbon felt has been investigated by Mohammadi et al. [25] for the electrocatalytic oxidation of methanol and a Co-based MOF/GO has been used by Mehek et al. [26] for ethanol electrooxidation. Ullah et al. [27] have reviewed some of the researches on the use of MOF-based materials for the electrocatalytic oxidation of methanol.

Poor electrical conductivity of most of MOF materials is the main limitation that may restrict their application in electrochemical processes. One strategy to solve this limiting problem is the integration of MOFs with carbon-based materials. This not only leads to enhanced conductivity, but also provides the composite materials with excellent characteristic performances attributed to the carbon-based nanostructures [28]. Improvement of electrocatalytic performances of MOF materials after incorporation with different carbon

nanostructures has been reported in several research papers [25-30]. In the present work, the synthesized Ni-BTC was composited with carbon nanotubes (CNTs) (Ni-BTC/CNTs). This caused the composite material to show higher electrocatalytic performance.

So far, the catalytic electro-oxidation of several small organic molecules such as methanol, ethanol, formaldehyde, ethylene glycol (EG), and etc. in ADAFCs have been explained. Among them, EG, due to its high electrochemical reactivity, high boiling point, inflammability, and easy handling/storage/transportation, can be an appealing choice for ADAFCs [31]. In the present paper, our group used a glassy carbon (GC) electrode as substrate. The efficiency of Ni-BTC/CNTs modified GC (Ni-BTC/CNTs-GC) electrode for the oxidation of EG was examined. The measurement results showed a high efficiency of Ni-BTC/CNTs toward the EG oxidation. This can be attributed to the structural advantages such as large surface area, highly porous nature of the Ni-MOF, and high electrocatalytic performances of Ni ion centers in Ni-BTC lattice combined with large surface area, high conductivity, and high electrochemical activity of CNTs.

2. EXPERIMENTAL SECTION

All chemicals were of analytical grade with the best quality assurance. The CNTs powder (length, 50 μm; inside diameter, 3–5 nm; outside diameter, 5–15 nm) was from US Research Nanomaterials, Inc.

The voltammetric electrochemical experiments were carried out using a PalmSens EmStat (PalmSens, The Netherlands) potentiostat. For the electrochemical experiment, a typical three-electrode system was used; a platinum plate was used as auxiliary/counter electrode, An Ag/AgCl (KCl 3 M) electrode was used as the reference electrode, and a modified glassy carbon (GC) electrode (0.02 mm diameter) with Ni-BTC (referred as GC/Ni-BTC) or Ni-BTC/CNTs (referred as GC/Ni-BTC/CNTs) was used as working electrode.

Ni-BTC, formulated $Ni_3(btc)_2 \cdot 12\ H_2O$, was prepared via a simple hydrothermal method. Briefly, 6 mmol of $Ni(NO_3)_2$ was dissolved into 7.5 mL deionized water. Another solution was prepared using 2 mmol of benzene-*1,3,5*-tricarboxylic acid in 7 mL *N,N*-dimethylformamide (DMF). Both the solutions were mixed together and then placed into a Teflon-lined autoclave and put into an oven at a temperature of 105°C for 48 h. After cooling to ambient temperature, the green crystals were collected, washed, and dried in air.

The Ni-BTC/CNTs composites were prepared by mixing different volumes of their dispersions in DMF. The dispersion of the Multi-walled CNTs was prepared by dispersing 10 mg of acid-treated CNT powder in 10 mL DMF using an ultrasonic bath. The dispersion of Ni-BTC powder in DMF (1 mg/mL) was prepared in the same way as that of CNTs dispersion. These two dispersions were then mixed together by different proportions and kept in the ultrasonic bath for 10 min to ensure homogenous suspensions of Ni-BTC/CNTs.

The modification of the GC electrode with the Ni-BTC or Ni-BTC/CNTs composites was done as follow: the GC electrode was first mechanically polished with alumina slurry. Then, after rinsing with doubly distilled water, the modified electrodes were simply prepared by drop-casting of appropriate volume of the Ni-BTC or Ni-BTC/CNTs dispersions on the electrode surface. the solvent was then evaporated under an infrared lamp. The prepared thin film-modified electrodes (GC/Ni-BTC, GC/Ni-BTC/CNTs) was utilized as working electrodes.

3. RESULTS AND DISCUSSION

3.1. SEM images of GC/Ni-BTC/CNTs and GC/Ni-BTC electrodes

Surface morphologies of the GC/Ni-BTC/CNTs and GC/Ni-BTC electrodes were examined by SEM. Figure 1A shows the surface of GC/Ni-BTC electrode and indicates that it consists of a large number of particles that are not uniform in shape and size but most of them are in the micrometer-scale. Figure 1B and Figure 1C show the SEM images taken from the surface of the GC/Ni-BTC/CNTs electrode at the same magnification of Figure 1A (Figure 1B) and at a higher magnification (Fig. 1C). From these figures, a uniform dispersion of CNTs can be clearly observed on the surface of the MOF. These observations prove the existence of strong interfacial interactions between CNTs and Ni-BTC particles such as π-π interactions between the aromatic rings of the side walls of CNTs and benzene rings of BTC ligands in the MOF structure. It causes the CNTs to be distributed more homogeneously in the composite that can give rise to the more effective improvements in some electrochemical properties of the composite.

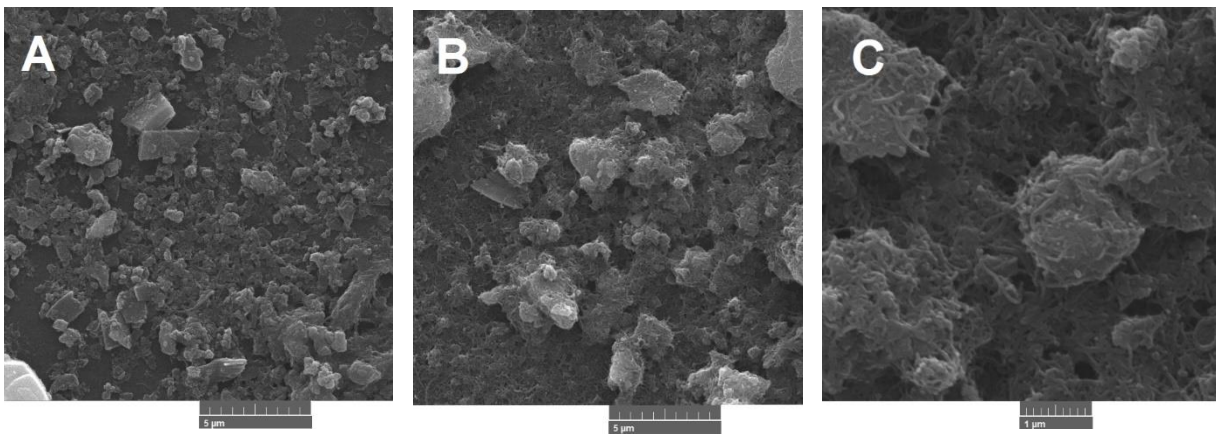

Figure 1. SEM images from the surface of GC/Ni-BTC (A), GC/Ni-BTC/CNTs (B), and GC/Ni-BTC/CNTs at a higher magnification (C)

3.2. Electrochemical properties of GC/Ni-BTC and GC/Ni-BTC/CNTs electrodes

Electrochemical behaviors of the GC/Ni-BTC and GC/Ni-BTC/CNTs electrodes were examined using cyclic voltammetry in 0.1 M NaOH supporting electrolyte solution. The results

are shown in Figure 2. The voltammograms were recorded after continuous cycling the electrode potential between 0.25 and 0.75 V at the scan rate of 100 mV s^{-1} up to observing a stable voltammogram (about 10 cycles). From curve a in Figure 2, for the GC/Ni-BTC/CNTs electrode, two peaks appeared in anodic and cathodic directions. The anodic peak at 0.55 V and the cathodic peak at 0.38 V could be related to the oxidation/reduction of the Ni^{2+}/Ni^{3+} couple. The mechanism is likely the same as that suggested for the zeolite-containing systems [34]. Some of Ni^{2+} cations of the Ni-BTC lattice surface undergo exchange with cations in the electrolyte solution followed by subsequent conversion of the exchanged Ni^{2+} cations into $Ni(OH)_2$. Therefore the redox process can be shown by the following mechanism [32,33]:

$$Ni(OH)_2 + OH^- \rightarrow NiOOH + H_2O + e^- \quad (1)$$

The MOF-modified electrode without CNTs (GC/Ni-BTC electrode) showed not well-defined peaks with smaller peak currents (curve b in Figure 2). This may be elucidated by considering the structure and properties of the CNTs. High conductivity as well as a large surface area of CNTs could provide the composite film with a large amount of electrocatalytic active sites, enhanced charge transfer kinetics, and improved electron transfer between Ni-BTC and the electrode substrate in the GC/Ni-BTC/CNTs electrode.

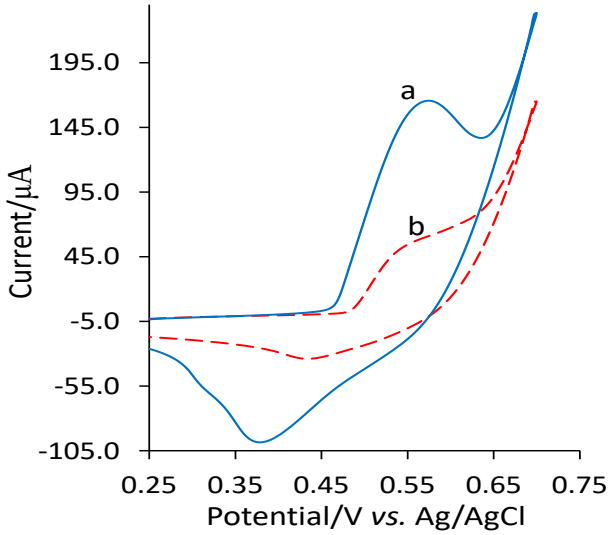

Figure 2. CVs of GC/Ni-BTC/CNTs (a) and GC/Ni-BTC (b) electrodes at the scan rate of 100 mV s^{-1} in 0.1 M NaOH

Figure 3 (A) shows the cyclic voltammograms obtained for the GC/Ni-BTC/CNTs electrode at different scan rates in the range of 5-500 mV s^{-1}. From this figure, anodic peak potential (E_{pa}) is slightly shifted toward more positive potentials while the cathodic one (E_{pc}) toward more negative values. This is also observed at some other Ni-based modified electrodes [12,32]. The corresponding plots of anodic (I_{pa}) and cathodic (I_{pc}) peak currents versus square root of the scan rate ($\upsilon^{½}$) are shown in Figure 3 (B) that represent ideal linear dependencies

between Ipa *vs.* $\upsilon^{1/2}$ and Ipc *vs.* $\upsilon^{1/2}$. This behavior is similar to those reported by other authors for Ni-based modified electrodes in alkaline solutions [12,32] and indicates the diffusion of OH^- ions from the solution toward the electrode, as the rate limiting step of the total charge transfer process of the modified electrode.

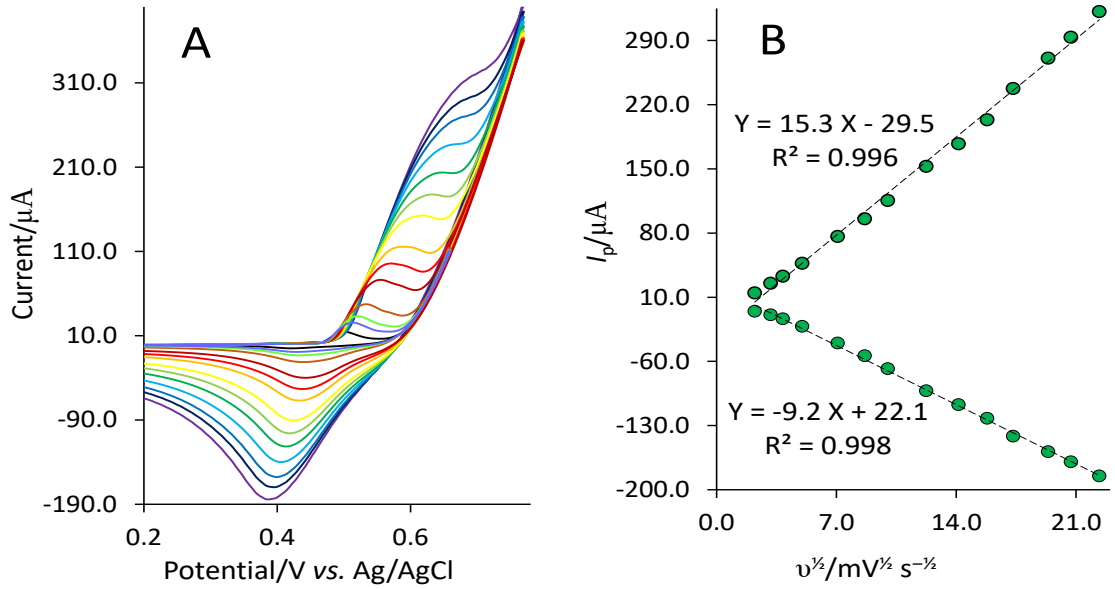

Figure 3. (A) CVs of GC/Ni-BTC/CNTs electrode at different scan rates (from inner to outer: 5, 10, 15, 25, 50, 75, 100, 150, 200, 250, 300, 375, 425, and 500 mV s^{-1}) and (B) the I_{pa} and I_{pc} *vs.* $\upsilon^{1/2}$ plots in 0.1 M NaOH solution

3.3. Oxidation of ethylene glycol at GC/Ni-BTC and GC/Ni-BTC/CNTs electrode

The CVs of the GC/Ni-BTC/CNTs electrode are shown in Figure 4. From this figure, in the presence of EG, the GC/Ni-BTC/CNTs electrode showed a remarkable increase in I_{pa} during the anodic scan and a slow decrease in I_{pc} during the backward scan. As reported in the literature [6,24,32,33], this behavior is typical of that observed for the catalytic Ni^{2+}/Ni^{3+}-mediated oxidation of EG. This can be presented as follows:

$$NiOOH + EG \rightarrow Ni(OH)_2 + products \quad (2)$$

Therefore, the catalytic oxidation of the EG at the modified electrode can be expressed based on the electrochemical (equation 1) catalytic chemical (equation 2) (EC′) mechanism. The oxidation of EG at the surface of the GC/Ni-BTC/CNTs electrode are also shown in the inset of Fig. 4 in comparison with that of the GC/Ni-BTC electrode. As expected, A remarkable increase in anodic current achieved for the electrooxidation of EG at the GC/Ni-BTC/CNTs electrode reflects its more effective surface area and enhanced electrocatalytic activity than that of the GC/Ni-BTC electrode. This obviously indicates that the combination of the CNTs with pure Ni-BTC can successfully enhance its electrochemical activity toward the EG oxidation.

The high electrical conductivity as well as the large surface area of CNTs can effectively improve the low electrical conductivity of the Ni-BTC, as one of the major drawbacks of Ni-based MOFs [28], while retain its advantages such as uniformly dispersed nickel active sites, high porosity, and large surface area.

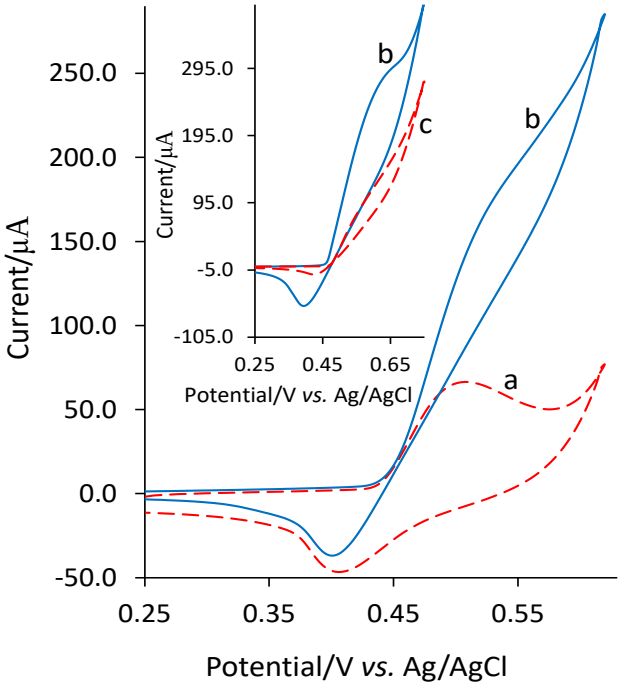

Figure 4. CVs at the GC/Ni-BTC/CNTs electrode (a) before and (b) after the addition of EG. The inset plot shows the CVs at the (b) GC/Ni-BTC/CNTs and (c) GC/Ni-BTC electrodes after the addition of EG in 0.1 M NaOH.

3.4. The effect of NaOH concentration

The NaOH concentration effect on the electrochemical response of the Ni-BTC/CNT-GC electrode was examined. The results of the cyclic voltammetry experiments that are conducted at different NaOH concentrations are shown in Figure 5. The ΔI values in this figure indicate the difference between the I_{pa} values of the voltammograms recorded in the presence and in the absence of EG. At the low NaOH concentrations, smaller and less well-defined peaks are observed as shown in inset A of Figure 5 (for 0.02 M NaOH). At the NaOH concentrations higher than 0.1 M, slightly larger and more well-defined peaks with higher ΔI values were observed. As the best results were achieved in 0.1 M NaOH (inset B of Figure 3), all the other experiments were conducted in 0.1 M NaOH.

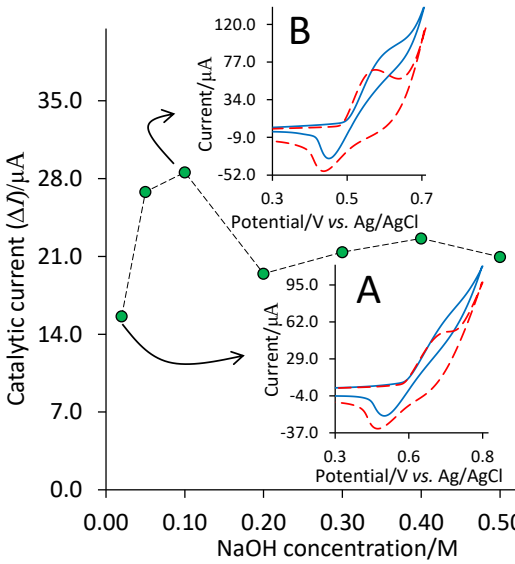

Figure 5. The catalytic current *vs.* NaOH concentration plot. Insets A and B show the CVs of GC/Ni-BTC/CNTs electrode before (dashed-line) and after (solid-line) the addition of EG in 0.02 M and 0.1 M solutions of NaOH, respectively

3.5. Optimization of the amount of Ni-BTC/CNTs dispersion

The effect of the volume of the Ni-BTC/CNTs dispersion used for the modification of the GC electrode on the catalytic current of EG was evaluated. The results are shown in Fig. 6. The highest ΔI value was achieved at 3 µL of the Ni-BTC/CNTs dispersion. Therefore, this volume was used as the optimum value of Ni-BTC/CNTs dispersion volume in all the remaining experiments. Slight decreases observed in the catalytic current at the higher volumes of dispersion (Figure 4) may be attributed to the effect of the thickness of the Ni-BTC/CNTs film. Increase in the film thickness causes a decrease in the film conductivity that results in reduction in peak current.

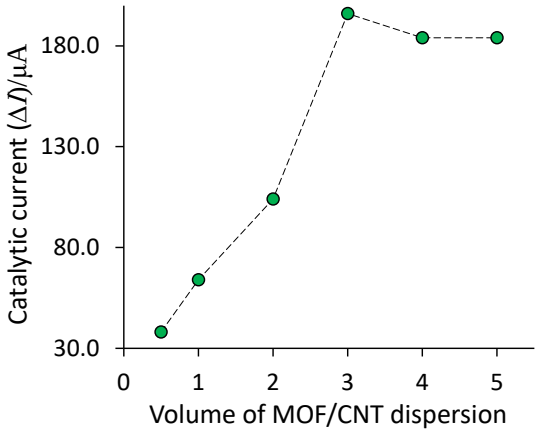

Figure 6. The catalytic current *vs.* Ni-BTC/CNTs dispersion volume used to modify the GC electrode surface by drop casting method

3.6. Optimization of the ratio of Ni-BTC/CNTs

In order to examine the effect of CNTs to Ni-BTC ratio on the electrocatalytic response, the GC/Ni-BTC/CNTs electrodes with different percent compositions of CNTs were prepared. The results are illustrated in Fig. 7. From this figure, the largest catalytic current can be achieved at the CNTs/Ni-BTC ratio of 1:10 (9.1 % percent composition of CNTs in Ni-BTC/CNTs composite). As can be expected, the combination of the CNTs with the pure Ni-BTC MOF improves the electrocatalytic performance properties but the CNTs-to-MOF ratios higher than about 1:10 leads to a decrease in catalytic current due to a decrease in the surface ratio of the MOF-to-Ni-BTC/CNTs. Hence, CNTs to Ni-BTC ratio of 1:10 ratio was chosen as the optimum ratio.

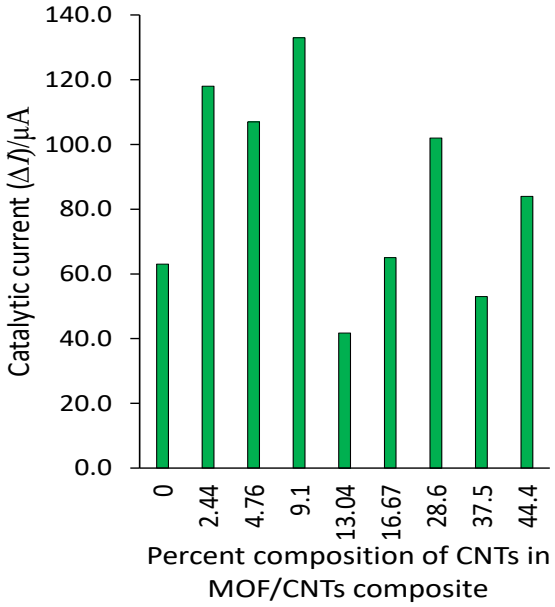

Figure 7. The catalytic current *vs.* percent composition of the CNTs in Ni-BTC/CNTs composite.

3.7. The effect of EG concentration

In order to investigate the effect of EG concentration, cyclic voltammograms of GC/Ni-BTC/CNTs electrodes for various concentrations of EG were recorded (Figure 8). The data shown in this figure indicate that EG can be efficiently electro-oxidized at the surface of the GC/Ni-BTC/CNTs electrode. It is clear that the oxidation current of EG is increased with the increase in concentration but it seems to level off at the concentrations beyond 0.02 M probably due to the active site saturation of the surface of the electrode. From these results, the optimum concentration for EG was found to be 0.02 M.

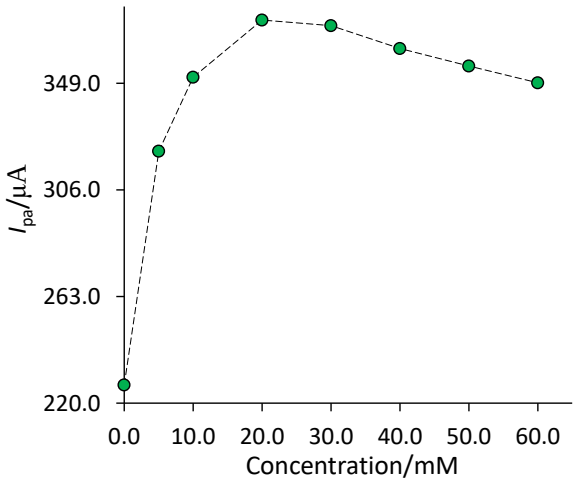

Figure 8. The plot of I_{pa} *vs.* the EG concentration

4. CONCLUSION

In this work, GC electrode surface was modified with a composite made from the Ni-BTC crystals and CNTs. The electrode was then applied for the oxidation of EG. Our results demonstrated that, under the optimized experimental parameters, the Ni-BTC/CNTs have good electrocatalytic performance for the electro-oxidation of EG. Also, the electrochemical measurements showed that it exhibited significantly higher electrocatalytic performance than pure GC/Ni-BTC electrodes, as a consequence of the high conductivity and large surface area of CNTs. The results prove that the Ni-BTC/CNTs composite can act as a promising electrocatalyst material for EG fuel cells.

Declarations of interest

The authors declare no conflict of interest in this reported work.

REFERENCES

[1] T. Matthews, S.P. Mbokazi, T.H. Dolla, S.S. Gwebu, K. Mugadza, K. Raseruthe, L.L. Sikeyi, K.A. Adegoke, O.D. Saliu, A.S. Adekunle, P. Ndungu, and N.W. Maxakato, Small Sci. 4 (2024) 2300057.

[2] P. Bishnoi, K. Mishra, S.S. Siwal, V.K. Gupta, and V.K. Thakur, Adv. Energy Sustainability Res. (2024) 2300266.

[3] E. Berretti, L. Osmieri, V. Baglio, H.A. Miller, J. Filippi, F. Vizza, M. Santamaria, S. Specchia, C. Santoro, and A. Lavacchi, Electrochem. Energy Rev. 6 (2023) 30.

[4] T. Eisa, H. O. Mohamed, Y.J. Choi, S.G. Park, R. Ali, M.A. Abdelkareem, S.E. Oh, and K.J. Chae, Int. J. Hydrogen Energy 45 (2020) 5948.

[5] G. S. Ferdowsi, S.A. Seyedsadjadi, and A. Ghaffarinejad, J. Nanostructure Chem. 15 (2015) 17.
[6] S. Awad, A.A.M. Al-Dies, R. Almahdawi, F.U. Y. Al-sheqefi, and E.E. Abdel-Hady, Polym. Adv. Technol. 35 (2024) e6322.
[7] F. Chen, S. Guo, S. Yu, C. Zhang, M. Guo, and C. Li, J. Colloid Interface Sci. 646 (2023) 43.
[8] S. S. Gupta, S. S. Mahapatra, and J. Datta, J. Power Sources 131 (2004) 169.
[9] A. Dutta, and D. Jayati, J. Phys. Chem. C 116 (2012) 25677.
[10] F. Fathirad, and E. Sadeghi, Fuel 358 (2024) 130130.
[11] F. Hassan, R. Naeem, S. Shabbir, S. Sharif, M. Mushtaq, and R. Sattar, New J. Chem. 48 (2024) 3614.
[12] Q. Lin, Y. Wei, W. Liu, Y. Yu, and J. Hu, Int. J. Hydrogen Energy 42 (2014) 1403.
[13] A. Nozad Golikand, M. Ghannadi Maragheh, L. Irannejad, and M. Asgari, Russ. J. Electrochem. 42 (2006) 167.
[14] M. Yavari, M. Mazloum-Ardakani, and A. Khoshroo, J. Nanostruct. 9 (2019) 268.
[15] T.Y. Zhang, X.Q. Wu, H.Y. Ruan, Y. Yuan, L. Wang, Y.P. Wu, Q.W. Han, R. Chi, and D.S. Li, Inorganica Chim. Acta 561 (2024) 121858.
[16] H.Y. Ruan, X.Q. Wu, T.Y. Zhang, Y. Yuan, L. Wang, Y.P. Wu, Q.W. Han, R. Chi, and D.S. Li, J. Solid State Chem. 330 (2024) 124460.
[17] S. Tanaka, K. Fuku, N. Ikenaga, M. Sharaf, and K. Nakagawa, Compounds 1 (2024) 141.
[18] A. Benny, K. R S. Devi, D. Pinheiro, and S.J. Chundattu, Results Chem. 7 (2024) 101414.
[19] J. Li, R. Li, W. Wang, K. Lan, and D. Zhao, Adv. Mater. (2024) 2311460.
[20] P. Q. Liao, J. Q. Shen, and J.P. Zhang, Coord. Chem. Rev. 373 (2018) 22.
[21] Y. Peng, S. Sanati, A. Morsali, and H. García, Angew. Chem. Int. Ed. 62 (2023) e202214707.
[22] N. Mushtaq, A. Ahmad, X. Wang, U. Khan, and J. Gao, Chem. Eng. J. 486 (2024) 150098.
[23] M. N. Lakhan, A. Hanan, Y. Wang, S. Liu, and H. Arandiyan, Langmuir 40 (2024) 2465.
[24] T. Noor, M. Ammad, N. Zaman, N. Iqbal, L. Yaqoob, and H. Nasir, Catal. Lett. 149 (2019) 3312.
[25] T. Mohammadi, M. G. Hosseini, H. Ashassi-Sorkhabi, and P. Yardani Sefidi, Synth. Met. 298 (2023) 117443.
[26] R. Mehek, N. Iqbal, T. Noor, H. Nasir, Y. Mehmood, and S. Ahmed, Electrochim. Acta 255 (2017) 195.
[27] N. Ullah, S. Ullah, S. Khan, D. Guziejewski, and V. Mirceski, Int. J. Hydrogen Energy 48 (2023) 3340.
[28] X. W. Liu, T. J. Sun, J. L. Hu, and S.D. Wang, J. Mat. Chem. A 10 (2016) 3584.

[29] T. Mohammadi, M.G. Hosseini, E. Pastor, and H. Ashassi-Sorkhabi, J. Energy Storage 79 (2024) 110146.
[30] E.T. Sayed, J.B.M. Parambath, M.A. Abdelkareem, H. Alawadhi, and A.G. Olabi, J. Alloys Compd. 976 (2024) 173194.
[31] L. An, and R. Chen, J. Power Sources 329 (2016) 484.
[32] M. Hadi, and H. Mostaanzadeh, Russ. J. Electrochem. 54 (2018) 1045.
[33] A. Salimi, M. Roushani, S. Soltanian, and R. Hallaj, Anal. Chem. 79 (2007) 7431.
[34] L.M. Muresan, Pure Appl. Chem. 83 (2010) 325.